communications earth & environment

Article

https://doi.org/10.1038/s43247-024-01639-6

Population at risk of dengue virus transmission has increased due to coupled climate factors and population growth

Taishi Nakase [1], Marta Giovanetti[2,3], Uri Obolski[4,5] & José Lourenço [6]

Dengue virus transmission has increased over the last four decades seemingly due to changes in climate, urbanization and population growth. Using estimates of dengue transmission suitability based on historical temperature and humidity data, we examined how shifts in these climatic variables and human population growth have contributed to the change in the geographical distribution and size of the global population living in areas with high climate suitability from 1979 to 2022. We found an expansion in climate suitability in North America, East Asia and the Mediterranean basin, where with few exceptions, endemicity is not yet established. Globally, we estimated that the population in areas with high climate suitability has grown by approximately 2.5 billion. In the Global South, this increase was largely driven by population growth in areas with historically favorable climate suitability, while in the Global North this increase predominantly occurred in previously unfavorable areas with limited population growth.

Dengue is the most common mosquito-borne viral disease globally, with an estimated 60 million symptomatic cases per year across 130 countries[1,2]. The dengue virus (DENV) is transmitted by *Aedes spp*. mosquitoes, which typically inhabit urban environments in tropical and subtropical regions. Disease burden in affected countries has greatly increased over the past few decades with Southeast Asia, South America, and the Western Pacific accounting for the majority of reported cases[1]. Dengue transmission is also suspected across much of Africa, where limited surveillance and the co-circulation of multiple mosquito-borne viruses make it difficult to estimate the true disease burden. Globally, the health and economic impact of dengue is substantial, with over 2 million disability adjusted life years worldwide[2] and an estimated annual total cost of US$2.1 billion and US$950 million in the Americas[3] and South-east Asia[4], respectively. In the last decade, the geographical range of dengue has also expanded to more temperate climates with the establishment of epidemic activity in parts of North America and a rise in autochthonous transmission in southern Europe[2,5]. Dengue has also become the leading cause of febrile illness among travelers returning from Southeast Asia[6], which has contributed towards the global spread of dengue into previously disease-free areas[7]. These recent trends are thought to be driven by changes in climate, land use, urbanization and human movement that increase proximity between vectors and humans and favor the spread of vector species[8].

The geographical range, timing and intensity of dengue transmission are influenced by the interaction between environmental factors such as temperature[9,10], humidity[11] and the presence of water sources[12], and anthropogenic factors such as urbanization[13,14] and population growth[14]. Climate strongly influences dengue transmission because it modulates several physical and behavioral traits of mosquitoes such as adult lifespan, aquatic developmental rates, viral incubation period and biting rate, thereby altering a mosquito's physiological potential to transmit the virus to new hosts[15,16]. In experimental studies of *Ae. aegypti* mosquitoes, higher temperature increased transmission potential through, for example, increases in mosquito lifespan[16] and decreases in viral incubation period[15]. At extreme temperatures, however, some mosquito traits such as survival are adversely affected[16]. At the same time, higher relative humidity has been shown to increase mosquito lifespan[17] and enhance virus propagation[18] in several

[1]Department of Epidemiology & Population Health, Stanford University School of Medicine, Stanford, CA, USA. [2]Instituto Rene Rachou, Fundação Oswaldo Cruz, Belo Horizonte, Minas Gerais, Brazil. [3]Department of Sciences and Technologies for Sustainable Development and One Health, Università Campus Bio-Medico di Roma, Rome, Italy. [4]Department of Epidemiology and Preventive Medicine, School of Public Health, Tel Aviv University, Tel Aviv, Israel. [5]Department of Environmental Sciences, Porter School of Environmental and Earth Sciences, Tel Aviv University, Tel Aviv, Israel. [6]Universidade Católica Portuguesa, Católica Medical School, Católica Biomedical Research Centre, Oeiras, Portugal. e-mail: jolourenco@ucp.pt

settings. *Ae. albopictus* mosquitoes, which has historically played a minor role in dengue transmission compared to *Ae. aegypti* mosquitoes, are better adapted to survive in more temperate climates[9]. Collectively, these climate-dependent variables have favored dengue transmission in warm and humid tropical regions and limited expansion into more temperate climates beyond the equatorial zone.

Using this accumulated experimental data on *Aedes spp.* mosquitoes[15,16,18], several studies have developed DENV suitability measures that mechanistically model the interactions between climate and mosquito-viral traits[9,19–22]. Mechanistic suitability measures vary in methodology and interpretation, but virtually all proposed approaches aim at quantifying transmission potential, often without resorting to epidemiological data which can be subject to reporting bias or have limited spatiotemporal resolution. Since climate imposes major constraints in mosquito survival and viral propagation, these mechanistic models can be useful in defining the geographical limits of transmission across both endemic and emerging areas. Additionally, these models can be easily designed to include non-linear relationships among mosquito-viral traits over various time scales and thus capture intra-annual fluctuations in transmission potential. Across diverse climate conditions, such models have been shown to accurately capture the timing and spatial distribution of reported dengue infections[20,23,24]. Many mechanistic modeling approaches, however, estimate dengue transmission potential on temperature-based relationships alone[9] or lack sufficient validation over diverse geographical areas. In contrast, statistical approaches including species distribution modeling that estimate associations between climate variables and dengue or vector observations are sometimes restricted in their ability to define the changing geographical limits or temporal dynamics of DENV transmission[25–27]. This can be attributed to spare reporting in areas where transmission is low[28] and difficulty capturing the nonlinear interactions between variables that mechanistically drive transmission[29]. Moreover, these statistical approaches often rely on a single minimum or maximum value to define climate-based limits, which may fail to account for more complex seasonal variation in transmission potential. Prior modeling efforts have also been developed on locally-specific parameter estimates with applications limited to specific regions[30–32]. Mechanistic dengue transmission suitability measures thus offer an effective way of examining how climate modulates the ecological constraints on dengue virus transmission at a higher spatial and temporal resolution. While improvements have been made in the estimation of future dengue risk with modeling techniques[25,26,33], the extent to which past environmental changes may have influenced the current geographical limits and epidemic activity of DENV has received less attention.

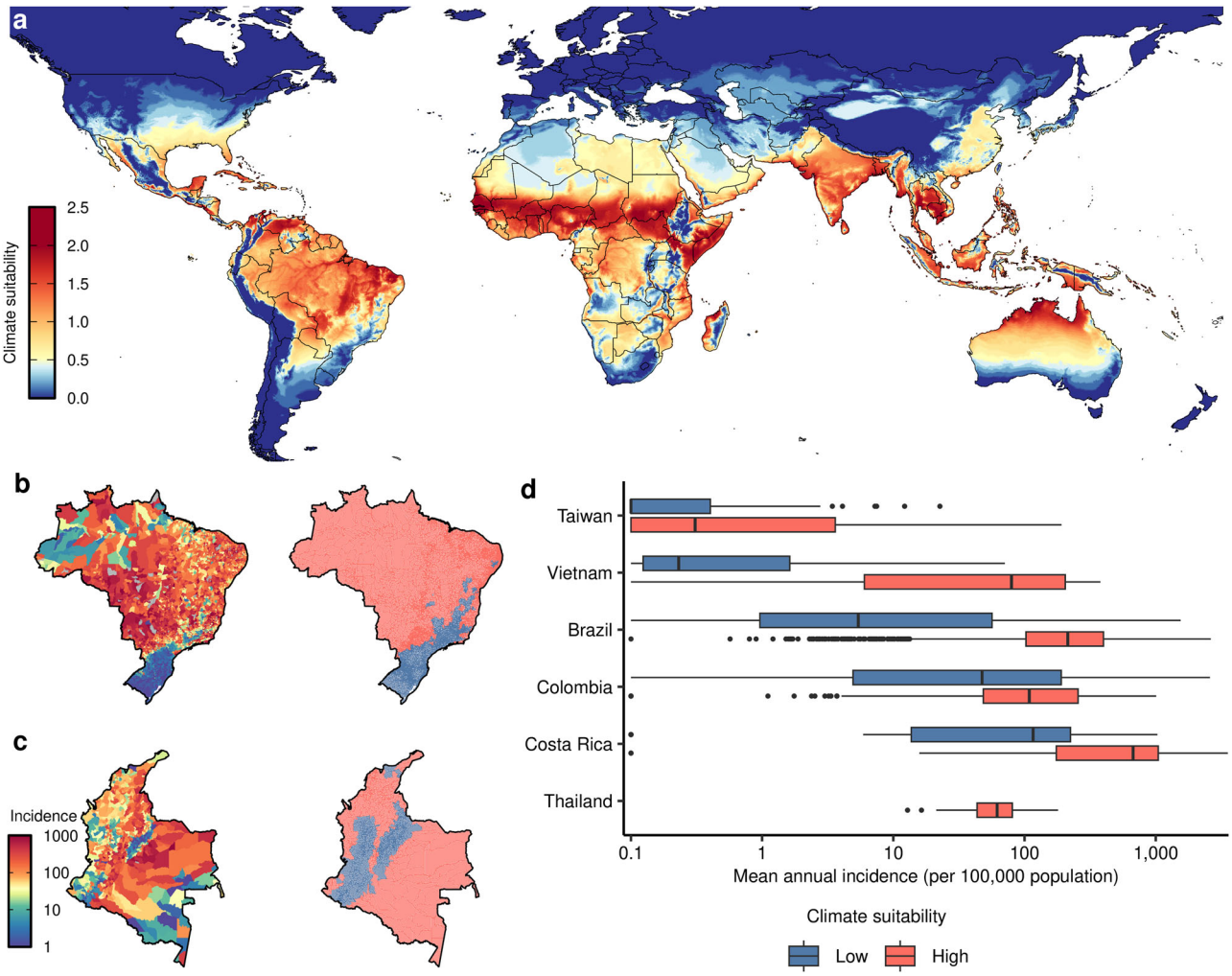

Fig. 1 | Climate suitability for dengue virus transmission. a Average climate suitability for dengue virus transmission between 1979 and 2022, presented on the Index P scale. **b**, **c** Mean yearly incidence (cases per 100,000 population; left panel) and mean annual climate suitability for dengue virus transmission (right panel) across municipalities in Brazil ($n = 5570$; 2000–2014) and Colombia ($n = 1119$; 2007–2017), respectively. Climate suitability is categorized into low (<0.5, blue) and high (≥0.5, red). Municipalities without incidence data are colored gray. **d** Comparison of mean annual incidence in low and high climate suitability regions across Taiwan (districts; $n = 368$; 1998–2020), Vietnam (provinces; $n = 63$; 1997–2010), Brazil (municipalities), Colombia (municipalities), Costa Rica (cantons; $n = 82$; 2012–2013, 2015–2017) and Thailand (provinces; $n = 77$; 2003–2022).

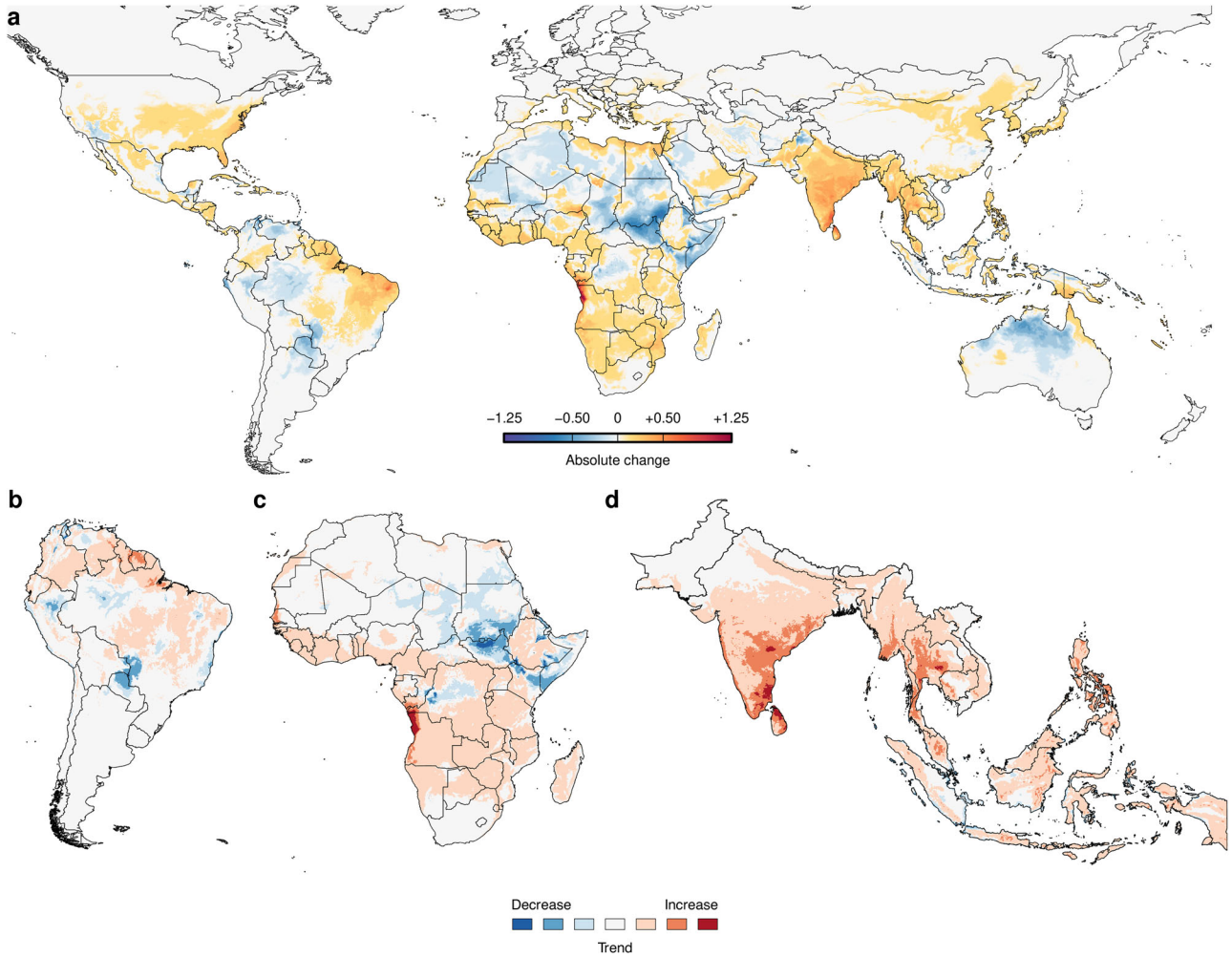

Fig. 2 | Historical changes in climate suitability for dengue virus transmission. **a** Absolute change in climate suitability on the Index P scale between 1979–1983 (past) to 2018–2022 (present). **b**–**d** Estimated trend in climate suitability for dengue virus transmission per pixel using monthly Index P time series from 1979 to 2022 for Africa, South America and South Asia/South-East Asia [dark blue = $(-\infty, -0.010]$, medium blue = $[-0.010, -0.005)$, light blue = $[-0.005, -0.0001)$, white = $[-0.0001, 0.0001)$, light orange = $[0.0001, 0.005)$, medium orange = $[0.005, 0.010)$, dark orange = $[0.010, \infty)$]. Pixels with trends that are not significant at an false discovery rate (FDR) < 0.10 are colored white.

In this study, we define climate-based DENV transmission suitability using Index P[20,23,24,34]. Index P is a mechanistic dengue suitability measure for *Ae. aegypti* mosquitoes based on temperature and relative humidity that has been shown to characterize the spatiotemporal dynamics of dengue transmission[23]. By leveraging publicly available estimates of Index P for 186 countries and territories from 1979 to 2022[35], we quantify local and global changes in climate suitability for DENV transmission over the last four decades at a monthly time resolution and at a spatial resolution of 360 arcseconds (approximately 11 km at the equator). For brevity, we refer to the interplay between temperature and relative humidity as climate, recognizing that climate is a complex phenomenon that accounts for additional meteorological variables. We then analyze how the distribution and size of human populations living in areas with high climate suitability for DENV transmission has changed over time and stratify these changes based on different factors including population density, income level and climate type that are known to be related to variation in dengue risk. We aimed to better understand how changes in climate (in terms of temperature and relative humidity) and population growth have contributed to the share of the global population living in areas with favorable environmental conditions for DENV transmission in different regions of the world.

Results

Global climate suitability for dengue virus transmission

Global variation in climate suitability for DENV transmission (hereafter referred to as climate suitability) was summarized using recently published spatiotemporal data for 186 countries or territories from 1979 to 2022[23,35] (Fig. 1a). In that work, a mechanistic mosquito-borne viral suitability measure referred to as Index P was used to estimate monthly time series of global climate suitability by *Ae. aegypti* mosquitoes based on satellite surface air temperature and relative humidity data. Although *Ae. albopictus* also transmits dengue virus, we focused on *Ae. aegypti* because it accounts for the majority of vector-human transmission[36], and it is the species for which detailed empirical data exist on the relationship between meteorological variables and vector-viral traits. These climate suitability estimates were previously validated as a measure of DENV transmission potential using dengue incidence data from Brazil, Thailand, Mexico and Puerto Rico[23]. We refer to Index P as a climate-based transmission suitability index recognizing that climate encompasses complex meteorological phenomena beyond temperature and relative humidity.

In this study, we present the average climate suitability per pixel from 1979 to 2022 (Fig. 1a). This summary metric highlights areas that remain suitable for transmission throughout the year and also accounts for areas

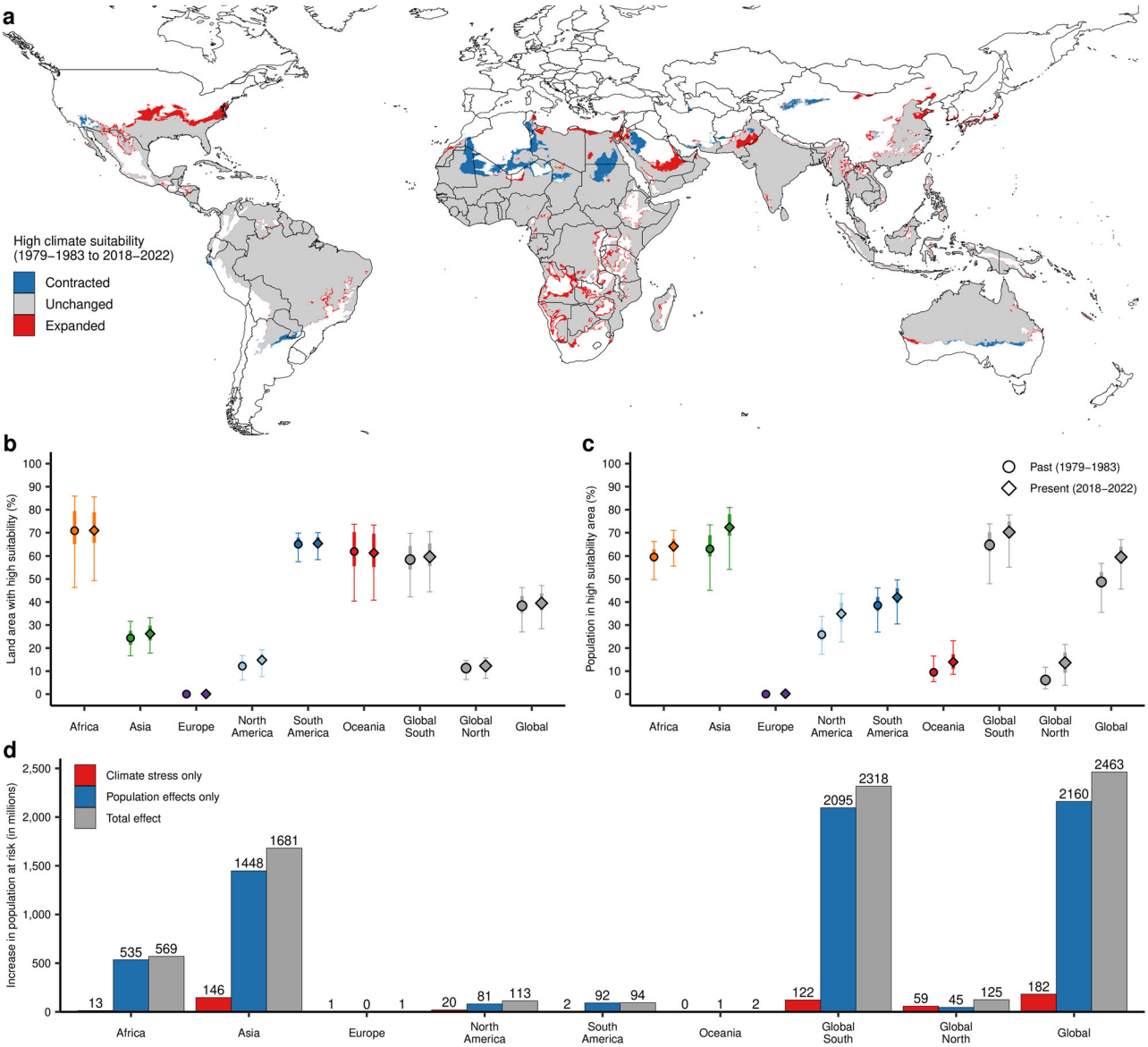

Fig. 3 | Estimated changes in land area and population with high climate suitability for dengue virus transmission. a Changes in areas classified as having high climate suitability for dengue virus transmission (using a threshold of 0.5). Areas that do not exceed the threshold for high climate suitability in either 1979–1983 or 2018–2022 are colored white. Estimated changes in land area (**b**) and population (**c**) with high climate suitability from 1979–1983 (circle) to 2018–2022 (diamond) for different regions. Mean (point), 50% (thick bar) and 90% (thin bar) credible intervals are shown. **d** Increase in the population (in millions) living in areas with high climate suitability from 1979–1983 to 2018–2022 due to climate effects (red), population effects (blue) and both climate and population effects (gray).

that are characterized by brief periods of very high transmission potential interspersed with periods of less favorable climate conditions. It should thus be interpreted as the potential for epidemic activity rather than endemic transmission. Climate suitability was highest within the tropical, subtropical and temperate areas around the equator. Visually, the spatial distribution of climate suitability was consistent with previous reports of global dengue incidence[2]. Specifically, high climate suitability was estimated across the western tropical zone of Africa, the Indian subcontinent, Southeast Asia, the Western Pacific, and Latin America, where DENV is known to be largely endemic and reported incidence is high[2]. Relatively high climate suitability was also estimated in areas where DENV has shown autochthonous transmission but is not yet known to be endemic (e.g., southern United States and northern Australia), or where infections are suspected to be under-reported due to limited surveillance (e.g., Central and Eastern Africa). Climate suitability was generally low across continental Europe with areas of non-zero suitability confined to isolated parts of Spain, France, Italy, and Turkey, where autochthonous cases have also been on the rise over the past decade.

Next, we used reported dengue case counts for several countries with dengue surveillance data to characterize the relationship between estimated climate suitability and observed dengue incidence (Fig. 1b–d). Using a threshold of 0.5 to define high climate suitability (see Technical validation of suitability index for details), areas of high climate suitability generally had higher dengue incidence than areas of low climate suitability across municipalities in Brazil (Fig. 1b) and Colombia (Fig. 1c). There were several municipalities in the Northwest of Brazil and the Southeast of Colombia where reported dengue case counts were lower than expected from the estimated climate suitability. It has been previously noted[35] that these municipalities form part of the Amazon rainforest, which may have lower reported dengue cases due to factors such as low population density, poor surveillance and limited connectivity between communities. Similar results were observed across Costa Rica, Vietnam and Taiwan, with higher dengue

incidence in high suitability areas than low suitability areas (Fig. 1d, Supplementary Fig. 1). There was notable variation in the absolute magnitude of dengue incidence across countries (Fig. 1d), which may reflect local differences in non-climatic factors that contribute to dengue transmission, including the levels of existing local herd-immunity.

To quantify the effect of climate suitability on dengue incidence, we fit a censored linear regression model for each country (except Thailand where all provinces had high climate suitability) with mean annual incidence as the outcome, climate suitability as a binary independent variable (high vs. low suitability), and population density and population size as covariates (Supplementary Fig. 2). Across 5566 municipalities in Brazil, we found that high suitability areas had a 37-fold (95% confidence interval = 33–42) greater incidence than low suitability areas. In Colombia, we observed a smaller effect with a 3-fold (95% confidence interval = 2–5) greater incidence in high vs. low suitability areas. We then meta-analyzed the results for each country using a random-effects model. Across the five countries, high climate suitability was associated with a 11-fold (95% confidence interval = 4–36) greater dengue incidence compared to low climate suitability (Supplementary Fig. 2).

Global changes in climate suitability for dengue virus transmission

We examined how climate suitability for DENV transmission has changed from 1979 to 2022. First, we defined past climate suitability as the average suitability from 1979 to 1983 and present climate suitability as the average suitability from 2018 to 2022 (Supplementary Fig. 3). We estimated the absolute change in climate suitability over the last 40 years by calculating the difference between the estimates of past (1979–1983) and present (2018–2022) suitability (Fig. 2a). Globally, we observed increases in climate suitability in the southern United States (Supplementary Fig. 4), northeastern Brazil, western and southern Africa, the Indian subcontinent, Southeast Asia and coastal areas of continental Europe (Supplementary Fig. 5). Decreases in climate suitability were observed in northern Australia (Supplementary Fig. 6), parts of South America and the northeast of Africa.

To account for transient climate variability and identify areas where climate suitability is exhibiting sustained changes over time, we quantified long-term trends in monthly time series of suitability per pixel using a seasonal Mann–Kendall test (Fig. 2b–d, Supplementary Fig. 7). Globally, we estimated that 28.5% of total land area (38.2 million km^2) exhibited long-term changes in climate suitability (FDR $q < 0.1$). Trends towards both higher and lower climate suitability were concentrated within the equatorial tropical and subtropical zones, coinciding with regions that have historically exhibited high climate suitability (Supplementary Fig. 8). In South America, Africa and Asia, we found that 37.4% (6.6 million km^2), 51.4% (15.3 million km^2) and 26.5% (11.8 million km^2) of total land area have shown sustained long-term changes in climate suitability from 1979 to 2022.

We then identified areas that transitioned from low to high suitability (i.e., expansion) and from high to low suitability (i.e., contraction) to understand how and where the geographical limits of high climate suitability (defined using a threshold of 0.5) have changed over the last 40 years (Fig. 3a). These estimates were based on the absolute change in suitability from 1979–1983 to 2018–2022 (Fig. 2a), and thus reflect the combined effects of short-term fluctuations and long-term trends in climate suitability. Globally, the proportion of land area with high climate suitability increased from 38.4% to 39.5% (Δ = 1.1 percentage points (pp), 90% credible interval (CI) = 0.9–1.4), corresponding to an expansion of approximately 1.5 million km^2. Similarly, the land area with favorable climatic conditions increased by 0.8 million km^2 from 24.4% to 26.2% (Δ = 1.8 pp, 90% CI = 1.4–2.2) in Asia and by 0.6 million km^2 from 12.2% to 14.8% (Δ = 2.6 pp, 90% CI = 1.5–3.1) in North America (Fig. 3b).

In Africa, expansion in climate suitability in Southern and Central Africa was accompanied by contraction in climate suitability in Northern and Western Africa (Supplementary Fig. 9), resulting in relatively little change in the total high-risk land area (Δ = 0.1 pp, 90% CI = −1.2–2.6). Locally, we observed large increases in climate suitability in Angola (Δ = 17.1 pp, +220,000 km^2), Namibia (Δ = 16.0 pp, +130,000 km^2) and the Democratic Republic of the Congo (Δ = 4.6 pp, +110,000 km^2; Supplementary Fig. 10a, Supplementary Table 1). Conversely, we estimated large decreases in climate suitability in Algeria (Δ = −14.8 pp, -350,000 km^2), Sudan (Δ = −9.0 pp, −170,000 km^2) and Mauritania (Δ = −15.0 pp, −160,000 km^2). In South America, Europe and Oceania, there was marginal change in the geographical limits of climate suitability with expansion confined to coastal areas of Spain, southern Turkey and southeastern Brazil.

Global change in human populations in high-risk areas

Next, we examined how human population growth coincided with the changes in the land area with high climate suitability by geographically overlaying global climate suitability with the population data and calculating the total population living in high-risk areas (i.e., pixels with climate suitability greater than 0.5) in 1979–1983 and 2018–2022 (Fig. 3c, Supplementary Fig. 10b). We estimated that the proportion of the global population living in high-risk areas increased from 48.8% to 60.0% (Δ = 10.8 pp, 90% CI = 10.0–11.8) from 1979–1983 to 2018–2022, resulting in 2.5 billion more people living in areas with high climate suitability for dengue transmission (Fig. 3d).

The majority of this trend was driven by changes in Africa where the proportion of the population in high-risk settings increased from 59.6% to 64.2% (Δ = 4.6 pp, 90% CI = 4.2–5.9) and in Asia where the proportion increased from 63.1% to 72.3% (Δ = 9.3 pp, 90% CI = 7.2–12.0; Fig. 3c). In absolute terms, these changes represent 569 million and 1.68 billion more people living in high-risk areas in Africa and Asia, respectively. In Asia, five countries (India, China, Pakistan, Indonesia, and Bangladesh) contributed over 80% of the estimated increase (Supplementary Table 2). In Africa, changes in Western Africa, especially Nigeria, were responsible for the greatest share of this increase (Supplementary Table 2).

The absolute change in the population living in high-risk areas was comparatively smaller across the Americas with an increase from 25.6% to 34.9% (Δ = 9.1 pp, 90% CI = 5.3–11.2) in North America (roughly 113 million more people), and from 38.6% to 42.1% (Δ = 3.5 pp, 90% CI = 3.1–3.8) in South America (roughly 94 million more people; Fig. 3c, d). In South America, we estimated that Brazil, Venezuela, Columbia, Ecuador and Bolivia had the largest increases in the population living in high-risk areas (Supplementary Table 2). Substantial changes were also estimated for countries across Central America and the Caribbean, including Haiti, Honduras, and the Dominican Republic, where the share of the population in highly favorable climate conditions increased by over 5 percentage points. (Supplementary Table 2).

To estimate the independent contribution of climate change and population growth to the observed increase in the population living in high-risk areas, we considered hypothetical scenarios in which climate and population effects were each held constant over the four decades (Fig. 3d). Globally, we found that population and climate effects independently contributed 2.16 billion and 182 million more people in high-risk areas, respectively. This observation held across continents (except Europe), with population growth responsible for at least 4-fold more people living in high-risk areas than that estimated for the effects of climate alone. Interestingly, when countries were divided into the Global North and Global South (Supplementary Table 3), we found that climate effects contributed more to the increase in the population in high-risk areas than population growth (59 million vs. 45 million) in the Global North (Fig. 3d).

When we accounted for the combined effects of climate change and population growth, we observed that the summation of the independent effect of each factor was marginally less than their combined effects (2.34 billion vs. 2.46 billion; Fig. 3d). This suggests that population growth frequently occurred in locations which have only recently exceeded the high suitability threshold. Furthermore, the greater increase in the proportion of the global population living in high-risk areas (from 48.8% to 60.0%; Fig. 3c) compared to the increase in the total high-risk land area (from 38.4% to 39.5%; Fig. 3d), indicates that population growth has also disproportionately occurred in areas with historically high climate suitability.

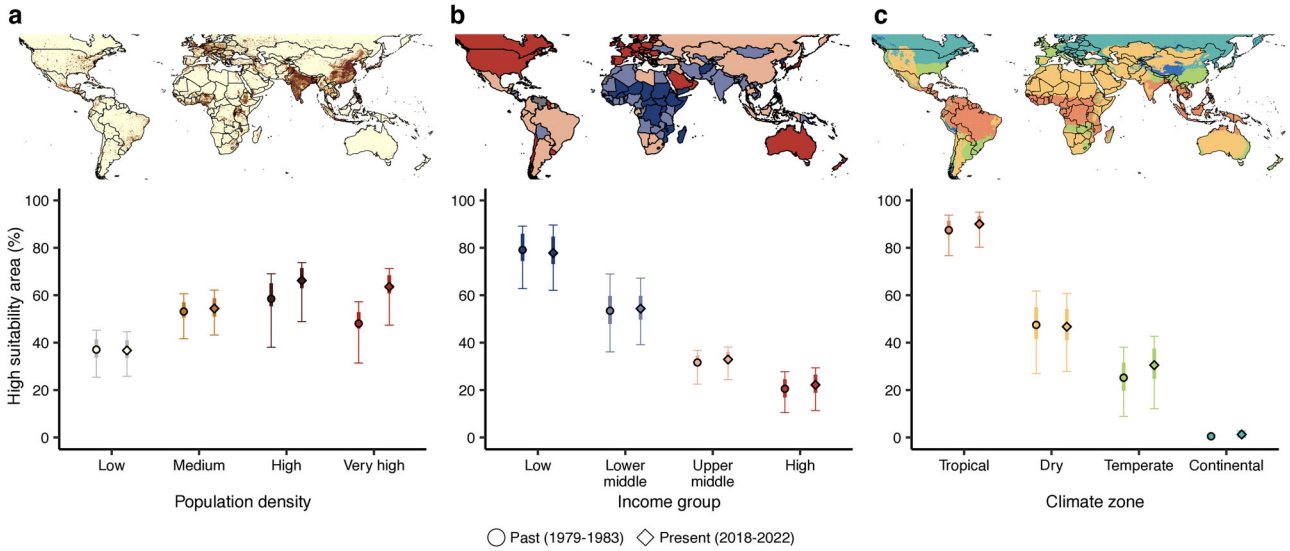

Fig. 4 | Shifts in the land area with high climate suitability for dengue virus transmission stratified by different variables. The proportion of land area with high climate suitability (using a threshold of 0.5) stratified by population density (**a**), economic income group (**b**), and climate zone (**c**) in 1979–1983 (circle) and 2017–2022 (diamond). The population density was categorized into low density (≤100 people/km^2, gray), medium density (101–300 people/km^2, light brown), high density (301–1500 people/km^2, dark brown) and very high density (≥ 1501 people/km^2, red). Income group was categorized into low (dark blue), lower middle (light blue), upper middle (light red) and high income (dark red) according to the World Bank classification of economies. Climate zone was defined according to the Köppen climate classification: tropical (orange), dry (yellow), temperate (green) and continental (blue). The polar zone was not included because it does not encompass any areas of high suitability. Mean (point), 50% (thick bar) and 90% (thin bar) credible intervals are shown.

Shifts in climate suitability stratified by different factors

Since *Ae. aegypti* prospers within densely-populated urban environments, we examined how climate suitability changed in areas with different human population density over the past 40 years (Fig. 4a). Globally, the proportion of high and very high density areas with high climate suitability for DENV transmission increased from 58.5% to 66.2% (Δ = 7.7 pp, 90% CI = 4.7–13.0) and from 48.1% to 63.6% (Δ = 15.5 pp, 90% CI = 14.1-–17.0), respectively. In contrast, the proportion of low and medium density areas with climate suitability were roughly unchanged over the last 40 years. Regionally, we estimated increases in the proportion of both high and very high density areas with high climate suitability across Asia, North America, South America and Oceania (Supplementary Fig. 11). Conversely, we estimated decreases in the proportion of high and very high density areas with high climate suitability across Africa, with increases limited to medium density areas.

To examine how the identified global shifts in climate suitability have been shared among different economies, we stratified the changes in climate suitability according to the World Bank income groups (Fig. 4b). Although lower income economies were estimated to have a greater proportion of favorable climate conditions, larger relative increases in climate suitability were observed for upper-middle and high income economies. Over the last four decades, the proportion of land area with high climate suitability increased from 31.6% to 32.9% (Δ = 1.3 pp, 90% CI = 0.2–2.4) and from 20.5% to 22.2% (Δ = 1.6 pp, 90% CI = 0.3–2.5) in upper-middle income and high income economies, respectively.

Finally, we asked whether the estimated changes in climate suitability were restricted to specific climate types using the Köppen–Geiger climate classification system (Fig. 4c). Interestingly, we found that temperate climate zones had the largest net change, with an increase in the proportion of land area with high climate suitability from 25.2% to 30.5% (Δ = 5.3 pp, 90% CI = 3.2–6.2). The tropical climate zones, which were estimated to have the greatest share of high climate suitability, had a smaller increase from 87.5% to 90.1% (Δ = 2.6 pp, 90% CI = 1.3–3.5).

Discussion

In this study, we used a dengue suitability measure that incorporates the effects of temperature and relative humidity on mosquito-viral traits to evaluate changes in climate suitability for DENV transmission at a global scale. We found that the equatorial tropical and subtropical zones spanning much of Sub-Saharan Africa, Southeast Asia, and northern South America experienced the largest increases in climate suitability over the past 40 years. We also observed an expansion in climate suitability to more temperate environments in North America, East Asia and the Mediterranean Basin. Critically, we found that the relative contribution of population growth and climate change to the share of the population living in areas with climate conditions favorable to DENV transmission was different in the Global South compared to the Global North. While the Global South experienced substantial population growth in historically high-suitability areas with comparatively minor changes in the total land area with high climate suitability, the Global North experienced a major expansion in the total land area with high climate suitability accompanied by relatively modest population growth. Together, these results highlight important differences in the potential drivers of increased dengue risk across different regions.

Globally, increases in climate suitability were found to be predominantly concentrated in areas that have historically exhibited both high climate suitability and epidemic activity, resulting in only marginal changes to the geographical limits of suitability. Several of the areas with marked increases in suitability have recently reported increased local transmission (e.g., southern United States[37] and Central Africa[28]) or larger and longer seasonal outbreaks (e.g., Central America[38]). In contrast to some future predictions of increased dengue risk in continental Europe[39], we found that climate suitability for DENV transmission has remained relatively low across Europe over the last 40 years, with increases in suitability confined to coastal areas in Spain, France, Italy and Turkey (Supplementary Fig. 5). Some of these areas, specifically Southern Spain, France and Northern Italy have seen a rise in short-term autochthonous transmission of dengue, chikungunya and West Nile virus over the past 5 years[39,40].

Interestingly, some regions, most notably Northern and Eastern Africa, were estimated to be decreasing in climate suitability. This suggests that the increasingly dry and warm conditions within and around this region may be negatively affecting mosquito-viral traits, resulting in decreased overall climate suitability for DENV transmission. These results point to a potentially ongoing, long-term shift in the geographical distribution of dengue risk with the emergence of DENV in new areas and its disappearance from

classically suitable areas in the future. This observation is consistent with future projections of dengue risk[26] and may follow the expected climate-driven decline in the transmission of malaria by the *Anopheles gambiae* mosquitoes, which are adapted to cooler conditions, in Africa[41,42]. However, many of these areas with decreasing suitability remain highly favorable for dengue transmission, emphasizing that climate-driven constraints on dengue transmission may not materialize for many years and are still subject to future climate change[43].

Additionally, we found that population growth has preferentially occurred in areas with historically high suitability, resulting in substantial increases in the population living in favorable climatic conditions. Assuming favorable conditions for the establishment of vector populations (e.g., suitable reproduction habitat), approximately 70% of the populations in Africa and Asia are currently living in areas with a high risk of infection—a roughly 15% increase relative to four decades earlier. Therefore, despite relatively small changes in the geographic limits of climate suitability, parallel population growth has resulted in millions of additional people living in areas with high climate suitability. This rapid growth in the available host population in climate-suitable areas emphasizes the increasing public health burden that the Global South will face as DENV continues to spread to new areas.

The increase in the proportion of high and very high human density areas with high climate suitability has implications for how we understand the recent increase in global dengue incidence. In a study on future dengue risk in Southeast Asia, it was found that high density areas, relative to both low and very high density areas, confer the highest risk of infection[33]. Taken together with their findings, our results point to the emergence of high density population centers as a potential contributor to the currently high risk of DENV transmission in many parts of the world. Additionally, many epidemiological studies from dengue-endemic areas in Southeast Asia have identified an association between poor urban planning (i.e., limited water infrastructure and waste management) and increased dengue transmission[44,45]. Hence, there is a need to more closely examine the link between urban development in high density areas and climate-based dengue risk. These links are likely to become increasingly important as the Global South, particularly Africa and South America, continues to undergo rapid urbanization and industrial development while facing higher climate suitability for DENV transmission.

There are several limitations as well as potential future opportunities of this study. Our model considers the empirical effects of temperature and humidity on transmission suitability, but other factors including precipitation[10,11], altitude[46], urbanization[44], and vegetation[10] could either constrain or favor local transmission. Furthermore, our suitability index does not provide any assurance that the mosquito vector, human host, or the virus are present. Although we have previously demonstrated that the index robustly reproduces spatiotemporal patterns of dengue incidence[23], high climate-based transmission suitability (i.e., Index P) should not be interpreted as a guarantee of dengue epidemic activity, but rather as the fulfillment of one of several criteria necessary for DENV transmission. For areas without reported dengue cases, our estimates of climate suitability can help identify hotspots where there is climate-based potential for introduction or where incidence might be under-reported due to insufficient surveillance. For example, we estimated high transmission suitability in Central Africa where *Ae. aegypti* is predicted to be widely disseminated[10] but reported cases remain low[28]. We also identify areas in Europe and North America with estimated increases in climate suitability that have recently witnessed viral introductions albeit with short-term transmission success. Conversely, large differences in estimated climate suitability and reported cases were observed in arid environments such as central Australia where suitable mosquito breeding habitats may be scarce (e.g., due to low precipitation). Similarly, differences between dengue reporting and climate suitability may arise in sparsely populated areas such as the Amazon in South America where barriers to human and viral mobility, as well as necessary human density for sustained transmission, likely limit the occurrence of chains of transmission.

The mathematical expressions for mosquito-viral traits used in our suitability index are based on experimental data from *Ae. aegypti* mosquitoes and do not account for the potential contribution of *Ae. albopictus* mosquitoes to DENV transmission. This would be relevant e.g., for southern Europe, where *Ae. albopictus* is now established but *Ae. aegypti* is not. Previous research has shown that adult *Ae. albopictus* have higher survival rates than *Ae. aegypti* and are better adapted to persist at higher latitudes[9,10]. Using these experimental results, Brady et al.[9] developed maps defining the current thermal limits of persistence for these two vectors. It could be informative to contrast the historical geographical distribution of transmission suitability for these vectors while including the influence of both temperature and humidity. However, currently available empirical data on mosquito-viral traits as a function of climate variables do not provide sufficient information to fully parameterize and robustly validate Index P specific for *Ae. albopictus*. We also note that *Ae. aegypti* mosquitoes can transmit other arboviruses including chikungunya[47], Zika[48], and yellow fever[49] that may have greater public health impact than DENV in some regions. For example, yellow fever epidemics are increasing in frequency and intensity in southern Brazil, where DENV transmission remains low[50].

In this study, we directly addressed the question of whether long-term changes in climate suitability from 1979 to 2022 were mediated by observed and sustained incremental changes in underlying climate conditions. However, this is not the only way that climate suitability for transmission may have changed in the recent past. For example, cyclic climate phenomena such as the El Niño Southern Oscillation, which is responsible for changes in atmospheric pressure and sea-surface temperature in the Pacific Ocean, can modulate climate variability at a large spatial scale[51]. Climate extremes associated with events such as heat waves, droughts and floods have been shown to influence DENV transmission potential through, for example, increases in vector abundance[30,52]. It is also becoming clear that DENV transmission can be affected by global teleconnections existing between local climate phenomena and climate variability elsewhere on the planet (e.g., local temperature anomalies are influenced by the Indian Ocean basin-wide index[53]). Modeling the interaction effects between long-term climate change trends, recurrent and extreme climate events and global teleconnection phenomena on DENV transmission potential is an important area of research that is only now starting to be explored[53].

It is worth noting that our estimates of climate suitability reflect the recent past and do not represent what will happen in the future. Given recent acceleration in global warming, projections of dengue risk based on climate change forecasts decades into the future may differ from our estimates of the historical distribution and magnitude of changes in climate suitability. Nevertheless, our results have implications for how current resources, including the recently developed TAK-003 dengue vaccine[54,55], should be distributed globally. We found that recent increases in the global population living in areas with high climate suitability have been concentrated in the Global South. Hence, immediate increases in DENV activity are expected in the Global South, especially in Asia and West Africa. This could influence the need to focus vaccination efforts on these locations. Such vaccination campaigns could also have an indirect effect on the Global North, by mitigating the impact of international travel from dengue-endemic regions as a source of viral introduction into dengue-free areas that have become more suitable for DENV transmission in recent years.

In this study, we aimed to better understand how the current epidemiology of dengue has been shaped by historical changes in climate suitability for DENV transmission and population growth. The reported outputs stand as a complement to a number of other studies focused on mapping the distribution of DENV vectors[10] and forecasting future transmission based on climate change projections[26,33]. Overall, we demonstrate that there has been a substantial increase in the global population living in areas with high climate suitability for DENV transmission. Critically, we showed that the processes that have facilitated this increase in the population in high-risk settings differed between the Global South and the Global North. In the Global South, this increase was predominantly driven by population growth, while in the Global North, it was driven by an expansion

in climate suitability to more temperate climates. Taken together, our results highlight distinct climate and population effects that are increasing DENV transmission suitability in both endemic and disease-free areas.

Methods

Dengue surveillance data

Data on yearly dengue case counts from 2000 to 2014 at administrative level-2 (municipalities) in Brazil were obtained from the Brazilian Information System for Notifiable Diseases (SINAN)[56]. SINAN collects information on cases of compulsorily notifiable diseases across all 26 states and the Federal District. It includes clinically suspected dengue infections without laboratory confirmation for 5570 municipalities. Four municipalities had incomplete data and were excluded from the analysis: Mojuí dos Campos (Pará), Pescaria Brava (Santa Catarina), Balneário Rincão (Santa Catarina), and Paraíso das Águas (Mato Grosso do Sul). Data on yearly dengue case counts from 1998 to 2022 at administrative level-1 (provinces) in Thailand were obtained from the Division of Epidemiology, Ministry of Public Health[57], which collates case notification data across all 77 provinces in a national disease surveillance system. Dengue case data for Colombia at administrative level-2 (municipalities) for 2007–2017 ($n = 1119$), Costa Rica at administrative level-2 (cantons) for 2012–2013 and 2015–2017 ($n = 82$), Taiwan at administrative level-2 (districts) for 1998–2020 ($n = 368$) and Vietnam at administrative level-1 (provinces) for 1997–2010 ($n = 63$) were obtained from OpenDengue[58,59], a database of dengue case counts from multiple publicly available sources. Full details on case definitions and data processing can be found in Clarke et al.[58]. Countries were selected for inclusion in this analysis if there were at least five years of dengue case data at a sufficiently high spatial resolution (administrative level-2 for larger countries and administrative level-1 for smaller countries).

Dengue transmission suitability index

We estimated climate suitability for DENV transmission using a previously published suitability measure referred to as Index P[20,34]. Index P estimates climate suitability for DENV transmission by *Ae. aegypti* mosquitoes using monthly temperature and relative humidity time series data within a mechanistic climate-based dengue transmission model. Spatiotemporal Index P data for 186 countries and territories from 1979 to 2022 were obtained from Nakase et al.[23,35]. This data is organized into global grid layers and includes Index P time series for pixels at a time resolution of 1 month (1979–2022) and a spatial resolution of 360 arcseconds (approximately 11 km at the equator). The methods and data for Index P estimation have been previously described in detail for all countries and territories[20,23].

Briefly, Index P is derived from a mechanistic model of dengue transmission potential (Eq. 1). It uses mathematical expressions for relationships between DENV-*Ae. aegypti* traits and meteorological variables (i.e., temperature (t) and relative humidity (u)) obtained from empirical studies to model the transmission potential of each female mosquito under conditions where susceptible hosts (h), the virus and its vectors (v) are assumed to be present. Climate-dependent functions of relevant epi-entomological parameters include extrinsic incubation period ($\gamma^{v}_{(t)}$), mosquito lifespan ($\mu^{v}_{(u,t)}$), mosquito biting rate ($a^{v}_{(u)}$), transmission probability per mosquito bite from infected human to susceptible mosquito ($\phi^{h\to v}_{(t)}$) and from infected mosquito to susceptible human ($\phi^{v\to h}_{(t)}$). Parameters that are assumed to be climate-independent include intrinsic incubation period (γ^{h}), human lifespan (μ^{h}) and human infectious period (σ^{h}). Each parameter is described by a probability distribution that is parameterized based on knowledge of the biology of the human hosts, *Ae. aegypti* vectors and dengue virus. Since the average intrinsic incubation period and infectious period are relatively short compared to the average human lifespan (i.e., days vs. years), variability in human lifespan has minimal effect on the magnitude of Index P and thus it is assumed to have the same distribution over time. Similarly, the probability distribution of each of the other climate-independent parameters is assumed to be the same over time and space. The probability distribution of each climate-dependent parameter varies according to the temperature and relative humidity of each pixel at each time point. Index P per pixel is estimated by sampling the distributions of each of the climate-dependent and climate-independent parameters at each time point and then using the sampled parameter values to calculate $P_{(u,t)}$ over time. The Index P dataset used in this study was estimated based on average monthly surface air temperature and relative humidity data from 1979 to 2022 obtained from Copernicus.eu[60] at a resolution of 360 arcseconds (approximately 11 km at the equator).

$$P_{(u,t)} = \frac{a^{v}_{(u)}{}^{2}\phi^{v\to h}_{(t)}\phi^{h\to v}_{(t)}\gamma^{v}_{(t)}\gamma^{h}}{\mu^{v}_{(u,t)}(\sigma^{h}+\mu^{h})(\gamma^{h}+\mu^{v}_{(u,t)})} \quad (1)$$

Demographic, economic and climate zone data

Global gridded population counts and population density for 1980 and 2020 were obtained from the Socioeconomic Data and Applications Center database[61,62] and the WorldPop database[63] at a resolution of 30 arcseconds (approximately 1 km at the equator). The population count data were aggregated to match the coarser spatial resolution of the suitability index data (360 arcseconds) by summing the population counts over 12 × 12 grids that match the spatial extent of the pixels of the gridded suitability index data. Similarly, the population density data were aggregated by averaging the population density values over the same grids. Aggregation of spatial data was performed using the *aggregate* function in the *raster* R package[64]. We assumed that the population data for 1980 reflected that for the period from 1979 to 1983, and that the population data for 2020 reflected that for the period from 2018 to 2022.

The economy of each country was categorized into income groups (low, low-middle, upper-middle and high) according to 2024 World Bank criteria[65]. The World Bank classifies each country into one of the four income groups using gross national income per capita, where low income economies are those with $1135 or less, lower middle-income are those between $1136 and $4465, upper middle-income are those between $4466 and $13,845 and high income are those with $13,846 or more. We assumed that the income category was uniform across the pixels within each country and equal to the country-level categorization. Income classification was not available for Venezuela, Western Sahara and Svalbard. The same income groups from the 2024 World Bank criteria were used for 1979–1983 and 2018–2022. The categorization of countries and territories into the Global South and Global North was obtained from the United Nations Finance Center for South-South Cooperation (Supplementary Table 3).

The Köppen–Geiger system was used to categorize pixels into climate zones[66]. The system aggregates global climatic variation into a simple classification scheme that reflects biome distributions around the world. The classification is based on the maximum, minimum and seasonality of air temperature and precipitation. There are five main climate zones: tropical, dry, temperate, continental and polar. The Köppen–Geiger climate classification data reflects the average of the period 1980–2016 at a resolution of 30 arcseconds. The gridded Köppen–Geiger climate data was resampled to the coarser spatial resolution of the suitability index data (i.e., 360 arcseconds) using a nearest neighbor technique, where the value of each pixel in the resampled data is set to the value of the nearest pixel in the original data. We assumed that the Köppen–Geiger climate classification was the same between 1979–1983 and 2018–2022.

An overview of the external datasets used in this study is provided in Supplementary Table 4.

Technical validation of suitability index

The Index P has been shown to be highly correlated with reported case data in several previous studies[20,24,34,67]. Detailed technical validation that supports the application of Index P to characterize local DENV transmission intensity and seasonality has also been performed previously for municipalities in Brazil (monthly from 2000–2014) and provinces in Thailand (monthly from 2007–2017)[23]. In this study, we extended those analyses and used yearly dengue case counts from Brazil (2000–2014), Colombia (1998–2022), Costa Rica (2012–2013, 2015–2017), Taiwan (1998–2020),

Thailand (2007–2017), and Vietnam (1997–2010). We focused on these countries because they span diverse climate conditions across Central America, South America and Asia, and have made publicly available high-resolution dengue case data.

First, we aggregated the Index P data to match the spatial resolution of the dengue case data by averaging the Index P values over all pixels that lie within the boundaries of each of the administrative units of each country. To quantify the relationship between Index P and DENV transmission, we then fit a separate tobit model for each country with log-transformed mean annual incidence (cases per 100,000 population) as the outcome and Index P as the binary independent variable (low vs. high suitability) with log-transformed population density and log-transformed population count as covariates. The Tobit model is a censored regression model that estimates a linear relationship when there is censoring in the outcome. We used the Tobit model to account for the left censoring of the dengue incidence data at zero. Index P was dichotomized into low and high suitability because it was previously shown that Index P and DENV incidence exhibit a nonlinear relationship, where incidence increases with Index P until reaching a plateau where incidence remains relatively constant despite increases in Index P[23]. We set the threshold for high climate suitability for DENV transmission at 0.5, which is the approximate value at which the start of the plateau was previously observed. Theoretically, an Index P of 0.5 corresponds to a mean basic reproduction number of 1 in a population where the average number of adult female mosquitoes per host is 2. The plateau at high Index P values is thought to reflect non-climatic factors such as accumulated herd immunity that constrain the size of epidemics. Finally, the country-level estimates were meta-analyzed in a random effects model with a restricted maximum likelihood estimator.

Summarization of suitability index

We estimated the past and present climate suitability for DENV transmission by calculating the average Index P for 1979–1983 and 2018–2022, respectively. For brevity, we refer to the time periods from 1979 to 1983 (i.e., the first five years of available data) and from 2018 to 2022 (i.e., last five years of available data) as the past and present respectively, recognizing that our dataset covers only the recent past over the last four decades. Uncertainty estimates for past and present climate suitability were estimated by sampling from the distribution of the spatiotemporal Index P data provided with the dataset from Nakase et al.[23,35]. We generated 1000 samples of the average Index P and calculated the 50% and 90% credible intervals based on the middle 50th and 90th percentiles of the estimated distribution of average Index P for 1979–1983 and 2018–2022.

Estimation of long-term trends in suitability index

Long-term climate suitability trends were estimated using the seasonal Mann–Kendall (MK) test[68] on the monthly Index P time series from 1979 to 2022. The MK test for trend detection is a non-parametric method based on rank that tests for the existence of a monotonic continuous trend in serially independent data. We use the seasonal extension of the MK test on the monthly Index P time series (528 data points for each pixel) to account for the observed seasonality in the transmission potential during a calendar year. We then used Sen's slope[26] to estimate the linear rate of change for each pixel. To reduce the impact of autocorrelation artifacts, we used the pre-whitening algorithm proposed by Yue et al.[69], which involves removing autocorrelation from detrended data. Briefly, the method consists of (1) estimating the slope on the original time series, (2) removing the estimated trend to detrend the time series, (3) removing the lag-1 autocorrelation from the detrended time series and (4) adding the trend back to the prewhitended time series. This algorithm accounts for potential autocorrelation while maintaining the power to detect significant trends. For each pixel, we applied the seasonal MK test on the prewhitended time series with statistical significance defined at a false discovery rate less than 0.10 across all pixels. Examples of the monthly Index P time series and corresponding trend estimates for two pixels are provided in Supplementary Fig. 12.

Estimation of climate and population effects on population in high suitability areas

The independent effect of changes in climate on the population living in areas with high suitability was estimated by holding the global population in 1980 constant and then allowing the climate suitability to change from 1979 to 2022. Similarly, the independent effect of changes in population size was estimated by holding the climate suitability in 1979–1983 constant and then allowing the global population to change from 1980 to 2020. The change in the population in high suitability areas was calculated by taking the difference between population in high suitability areas in 2020 and the population in high suitability areas in 1980.

Reporting summary

Further information on research design is available in the Nature Portfolio Reporting Summary linked to this article.

Data availability

The gridded spatiotemporal data of climate-based dengue virus transmission suitability from 1979 to 2022 at a time resolution of 1 month and a spatial resolution of 360 arcseconds are publicly available on figshare (https://doi.org/10.6084/m9.figshare.21502614.v5)[35]. Estimated long-term trends in climate suitability for dengue virus transmission at a spatial resolution of 360 arcseconds in addition to Supplementary Tables 1–3 have been made available on figshare (https://doi.org/10.6084/m9.figshare.26129593). Global gridded population counts and population density for 1980 and 2020 at a spatial resolution of 30 arcseconds were obtained from the Socioeconomic Data and Applications Center (SEDAC; https://sedac.ciesin.columbia.edu)[61,62] and WorldPop (https://www.worldpop.org)[63] databases. Dengue case counts for Brazil, Colombia, Taiwan, Costa Rica, Thailand and Vietnam were obtained from the Brazilian Information System for Notifiable Diseases (SINAN; http://portalsinan.saude.gov.br/)[56], Ministry of Public Health in Thailand (http://doe.moph.go.th/surdata/index.php)[57] and OpenDengue (https://opendengue.org)[58,59].

Code availability

All analyses were performed using R statistical software version 4.2.1. A brief tutorial on how to access, process and visualize the spatiotemporal maps of climate-based dengue virus transmission suitability is publicly available on GitHub (https://github.com/TaishiNakase/Index-P-estimation-and-applications). Code for the estimation of trends in climate suitability for dengue virus transmission and summarization of past or present climate suitability have been made available on GitHub (https://github.com/TaishiNakase/Global_IndexP_Trends).

Received: 17 January 2024; Accepted: 21 August 2024;
Published online: 30 August 2024

References

1. Stanaway, J. D. et al. The global burden of dengue: an analysis from the Global Burden of Disease Study 2013. *Lancet Infect. Dis.* **16**, 712–723 (2016).
2. Yang, X., Quam, M. B. M., Zhang, T. & Sang, S. Global burden for dengue and the evolving pattern in the past 30 years. *J. Travel Med.* **28**, taab146 (2021).
3. Halasa, Y. A., Zambrano, B., Shepard, D. S., Dayan, G. H. & Coudeville, L. Economic impact of dengue illness in the Americas. *Am. J. Trop. Med. Hyg.* **84**, 200–207 (2011).
4. Shepard, D. S., Undurraga, E. A. & Halasa, Y. A. Economic and disease burden of dengue in Southeast Asia. *PLoS Negl. Trop. Dis.* **7**, e2055 (2013).
5. Cassaniti, I. et al. Preliminary results on an autochthonous dengue outbreak in Lombardy Region, Italy, August 2023. *Euro Surveill.* **28**, 2300471 (2023).

6. Schwartz, E. et al. Seasonality, annual trends, and characteristics of dengue among Ill returned travelers, 1997–2006. *Emerg. Infect. Dis.* **14**, 1081–1088 (2008).
7. Quam, M. B. et al. Estimating air travel–associated importations of dengue virus into Italy. *J. Travel Med.* **22**, 186–193 (2015).
8. Franklinos, L. H. V., Jones, K. E., Redding, D. W. & Abubakar, I. The effect of global change on mosquito-borne disease. *Lancet Infect. Dis.* **19**, e302–e312 (2019).
9. Brady, O. J. et al. Global temperature constraints on Aedes aegypti and Ae. albopictus persistence and competence for dengue virus transmission. *Parasites Vectors* **7**, 338 (2014).
10. Kraemer, M. U. G. et al. The global distribution of the arbovirus vectors Aedes aegypti and Ae. Albopictus. *eLife* **4**, e08347 (2015).
11. de Oliveira Custódio, J. M. et al. Abiotic factors and population dynamic of Aedes aegypti and Aedes albopictus in an endemic area of dengue in Brazil. *Rev. Inst. Med. Trop. São Paulo* **61**, 18 (2019).
12. Foo, L., Lim, T., Lee, H. & Fang, R. Rainfall, abundance of Aedes aegypti and dengue infection in Selangor, Malaysia. *Southeast Asian J. Trop. Med. Public Health* **16**, 560–568 (1985).
13. Lee, S. A., Economou, T., de Castro Catão, R., Barcellos, C. & Lowe, R. The impact of climate suitability, urbanisation, and connectivity on the expansion of dengue in 21st century Brazil. *PLoS Negl. Trop. Dis.* **15**, e0009773 (2021).
14. Struchiner, C. J., Rocklöv, J., Wilder-Smith, A. & Massad, E. Increasing dengue incidence in Singapore over the past 40 years: population growth, climate and mobility. *PLoS One* **10**, e0136286 (2015).
15. Chan, M. & Johansson, M. A. The incubation periods of dengue viruses. *PLoS One* **7**, e50972 (2012).
16. Brady, O. J. et al. Modelling adult Aedes aegypti and Aedes albopictus survival at different temperatures in laboratory and field settings. *Parasit. Vectors* **6**, 351 (2013).
17. Yé, Y., Louis, V. R., Simboro, S. & Sauerborn, R. Effect of meteorological factors on clinical malaria risk among children: an assessment using village-based meteorological stations and community-based parasitological survey. *BMC Public Health* **7**, 101 (2007).
18. Thu, H., Aye, K. & Thein, S. The effect of temperature and humidity on dengue virus propagation in Aedes aegypti mosquitos. *Southeast Asian J. Trop. Med. Public Health* **29**, 280–284 (1998).
19. Mordecai, E. A. et al. Detecting the impact of temperature on transmission of Zika, dengue, and chikungunya using mechanistic models. *PLoS Negl. Trop. Dis.* **11**, e0005568 (2017).
20. Obolski, U. et al. MVSE: an R-package that estimates a climate-driven mosquito-borne viral suitability index. *Methods Ecol. Evol.* **10**, 1357–1370 (2019).
21. Hamlet, A. et al. The seasonal influence of climate and environment on yellow fever transmission across Africa. *PLoS Negl. Trop. Dis.* **12**, e0006284 (2018).
22. Smith, D. L. et al. Ross, Macdonald, and a theory for the dynamics and control of mosquito-transmitted pathogens. *PLoS Pathog.* **8**, e1002588 (2012).
23. Nakase, T., Giovanetti, M., Obolski, U. & Lourenço, J. Global transmission suitability maps for dengue virus transmitted by Aedes aegypti from 1981 to 2019. *Sci. Data* **10**, 275 (2023).
24. Adelino, T. É. R. et al. Field and classroom initiatives for portable sequence-based monitoring of dengue virus in Brazil. *Nat. Commun.* **12**, 2296 (2021).
25. Bhatt, S. et al. The global distribution and burden of dengue. *Nature* **496**, 504–507 (2013).
26. Messina, J. P. et al. The current and future global distribution and population at risk of dengue. *Nat. Microbiol.* **4**, 1508–1515 (2019).
27. Hales, S., De Wet, N., Maindonald, J. & Woodward, A. Potential effect of population and climate changes on global distribution of dengue fever: an empirical model. *Lancet* **360**, 830–834 (2002).
28. Gainor, E. M., Harris, E. & LaBeaud, A. D. Uncovering the burden of dengue in Africa: considerations on magnitude, misdiagnosis, and ancestry. *Viruses* **14**, 233 (2022).
29. Campbell, K. M., Lin, C. D., Iamsirithaworn, S. & Scott, T. W. The complex relationship between weather and dengue virus transmission in Thailand. *Am. J. Trop. Med. Hyg.* **89**, 1066–1080 (2013).
30. Nosrat, C. et al. Impact of recent climate extremes on mosquito-borne disease transmission in Kenya. *PLoS Negl. Trop. Dis.* **15**, e0009182 (2021).
31. Bouzid, M., Colón-González, F. J., Lung, T., Lake, I. R. & Hunter, P. R. Climate change and the emergence of vector-borne diseases in Europe: case study of dengue fever. *BMC Public Health* **14**, 781 (2014).
32. Faridah, L. et al. Temporal correlation between urban microclimate, vector mosquito abundance, and dengue cases. *J. Med. Entomol.* **59**, 1008–1018 (2022).
33. Colón-González, F. J. et al. Projecting the future incidence and burden of dengue in Southeast Asia. *Nat. Commun.* **14**, 5439 (2023).
34. Perez-Guzman, P. N. et al. Measuring mosquito-borne viral suitability in Myanmar and implications for local Zika virus transmission. *PLoS Curr.* **28**, 10:ecurrents.outbreaks.7a6c64436a3085ebba37e5329ba169e6 (2018).
35. Nakase, T. & Lourenco, J. Global climate-driven transmission suitability maps for dengue virus transmitted by Aedes aegypti mosquitoes from 1979 to 2022. figshare https://doi.org/10.6084/M9.FIGSHARE.21502614.V5 (2023).
36. Simmons, C. P., Farrar, J. J., Van Vinh Chau, N. & Wills, B. Dengue. *N. Engl. J. Med*. **366**, 1423–1432 (2012).
37. Rivera, A. et al. Travel-associated and locally acquired dengue cases —United States, 2010–2017. *Mmwr. Morb. Mortal. Wkly. Rep.* **69**, 149–154 (2020).
38. Cafferata, M. L. et al. Dengue epidemiology and burden of disease in Latin America and the Caribbean: A Systematic Review of the Literature and Meta-Analysis. *Value Health Regional Issues* **2**, 347–356 (2013).
39. Liu-Helmersson, J., Rocklöv, J., Sewe, M. & Brännström, Å. Climate change may enable Aedes aegypti infestation in major European cities by 2100. *Environ. Res.* **172**, 693–699 (2019).
40. European Centre for Disease Prevention and Control & Control. *Dengue. In: ECDC. Annual Epidemiological Report for 2021*. (2023).
41. Bhatt, S. et al. The effect of malaria control on Plasmodium falciparum in Africa between 2000 and 2015. *Nature* **526**, 207–211 (2015).
42. Mordecai, E. A. et al. Thermal biology of mosquito-borne disease. *Ecol. Lett.* **22**, 1690–1708 (2019).
43. Kaye, A. et al. The impact of climate change and natural climate variability on the global distribution of *Aedes aegypti*. Preprint at https://doi.org/10.1101/2023.08.31.23294902 (2023).
44. Ooi, E.-E. & Gubler, D. J. Dengue in Southeast Asia: epidemiological characteristics and strategic challenges in disease prevention Dengue no Sudeste Asiático: características epidemiológicas e desafios estratégicos na prevenção da doença. *Cad. de. saúde. pública* **25**, S115–S124 (2009).
45. Wilcox, B. A., Gubler, D. J. & Pizer, H. F. Urbanization and the social ecology of emerging infectious diseases. In *The Social Ecology of Infectious Diseases* 113–137 (Elsevier, 2008). https://doi.org/10.1016/B978-012370466-5.50009-1.
46. Dhimal, M. et al. Risk Factors for the Presence of Chikungunya and Dengue Vectors (Aedes aegypti and Aedes albopictus), Their Altitudinal Distribution and Climatic Determinants of Their Abundance in Central Nepal. *PLoS Negl. Trop. Dis.* **9**, e0003545 (2015).
47. De Souza, W. M. et al. Chikungunya: a decade of burden in the Americas. *Lancet Reg. Health Am.* **30**, 100673 (2024).
48. Lessler, J. et al. Assessing the global threat from Zika virus. *Science* **353**, aaf8160 (2016).

49. Jentes, E. S. et al. The revised global yellow fever risk map and recommendations for vaccination, 2010: consensus of the Informal WHO Working Group on Geographic Risk for Yellow Fever. *Lancet Infect. Dis.* **11**, 622–632 (2011).
50. Giovanetti, M. et al. Genomic epidemiology unveils the dynamics and spatial corridor behind the Yellow Fever virus outbreak in Southern Brazil. *Sci. Adv.* **9**, eadg9204 (2023).
51. Wolter, K., Dole, R. M. & Smith, C. A. Short-Term Climate Extremes over the Continental United States and ENSO. Part I: Seasonal Temperatures. *J. Clim.* **12**, 3255–3272 (1999).
52. Gubler, D. J. et al. Climate variability and change in the United States: potential impacts on vector- and rodent-borne diseases. *Environ. Health Perspect.* **109**, 223–233 (2001).
53. Chen, Y. et al. Indian Ocean temperature anomalies predict long-term global dengue trends. *Science* **384**, 639–646 (2024).
54. Tricou, V. et al. Long-term efficacy and safety of a tetravalent dengue vaccine (TAK-003): 4·5-year results from a phase 3, randomised, double-blind, placebo-controlled trial. *Lancet Glob. Health* **12**, e257–e270 (2024).
55. Wilder-Smith, A. TAK-003 dengue vaccine as a new tool to mitigate dengue in countries with a high disease burden. *Lancet Glob. Health* **12**, e179–e180 (2024).
56. Brazilian Ministry of Health. Sistema de Informação de Agravo de Notificação (SINAN). http://portalsinan.saude.gov.br/ (2016).
57. Department of Disease Control, Ministry of Public Health. National Disease Surveillance (Report 506). http://doe.moph.go.th/surdata/index.php (2024).
58. Clarke, J. et al. A global dataset of publicly available dengue case count data. *Sci. Data* **11**, 296 (2024).
59. Clarke, J. et al. OpenDengue: data from the OpenDengue database. figshare https://doi.org/10.6084/M9.FIGSHARE.24259573 (2023).
60. Hersbach, H. et al. Essential climate variables for assessment of climate variability from 1979 to present. Copernicus Climate Change Service (C3S) Data Store (CDS) (2018).
61. Center For International Earth Science Information Network-CIESIN-Columbia University. Global Population Count Grid Time Series Estimates. https://doi.org/10.7927/H4CC0XNV (2016).
62. Center for International Earth Science Information Network - CIESIN - Columbia University. *Foresight Project on Migration and Global Environmental Change, Report MR4: Estimating Net Migration by Ecosystem and by Decade,1970–2010* (2011).
63. WorldPop. Global 100m Population total adjusted to match the corresponding UNPD estimate. https://doi.org/10.5258/SOTON/WP00660 (2020).
64. Hijmans R. raster: Geographic Data Analysis and Modeling. R package version 3.6-28, https://github.com/rspatial/raster (2024).
65. World Bank. World Bank Country and Lending Groups. https://datahelpdesk.worldbank.org/knowledgebase (2024).
66. Beck, H. E. et al. Present and future Köppen-Geiger climate classification maps at 1-km resolution. *Sci. Data* **5**, 180214 (2018).
67. Petrone, M. E. et al. Asynchronicity of endemic and emerging mosquito-borne disease outbreaks in the Dominican Republic. *Nat. Commun.* **12**, 151 (2021).
68. Hirsch, R. M., Slack, J. R. & Smith, R. A. Techniques of trend analysis for monthly water quality data. *Water Resour. Res.* **18**, 107–121 (1982).
69. Yue, S., Pilon, P., Phinney, B. & Cavadias, G. The influence of autocorrelation on the ability to detect trend in hydrological series. *Hydrol. Process.* **16**, 1807–1829 (2002).

Acknowledgements

The authors acknowledge that they received no funding in support of this research.

Author contributions

Conceptualization: T.N. and J.L. Methodology: T.N., U.O., and J.L. Investigation and Visualization: T.N. Writing and editing the manuscript: T.N., M.G., U.O., and J.L.

Competing interests

The authors declare no competing interests.

Additional information

Supplementary information The online version contains supplementary material available at https://doi.org/10.1038/s43247-024-01639-6.

Correspondence and requests for materials should be addressed to José. Lourenço.

Peer review information *Communications Earth & Environment* thanks the anonymous reviewers for their contribution to the peer review of this work. Primary Handling Editors: Paula Prist and Martina Grecequet. A peer review file is available.